



Low Density Polyethylene/Organoclay Nanocomposites Manufactured Using Oxidized Polyethylene as a Coupling Agent and the Flame Retardant Additive

Haydar U. Zaman*, Ruhul A. Khan

Institute of Radiation and Polymer Technology, Bangladesh Atomic Energy Commission, P.O. Box 3787, Savar, Dhaka, BANGLADESH

*Corresponding author e-mail: haydarzaman07@gmail.com

ARTICLE INFO

ABSTRACT

Article history:

Received: 23 August, 2021

Revised: 25 February, 2021

Accepted: 9 March, 2022

Available online: xx May, 2022

DOI: xxxxxxxxxxxxxxxxxxxxxx

Keywords: low density polyethylene, oxidized polyethylene, organoclay, mechanical properties, flame retardant properties

Low-density polyethylene (LDPE)/organoclay (cloisite 20A, abbreviation: C20A) nanocomposites were melted in this exploration by intercalation technique with low molecular weight oxidized polyethylene (OxPE) as a coupling agent. The effects of OxPE on morphology, mechanical, thermal, flame retardant properties were identified by transmission electron microscopy (TEM), X-ray diffraction (XRD), tensile test, differential scanning calorimetry (DSC), and flammable tests, respectively. XRD and TEM results exhibited that the interlayer distance of the nanoparticle layers were increased and a partial intercalated structure was prepared with an intercalated technique. Mechanical experiments exhibited that the inclusion of 5 wt% C20A in LDPE was significantly improved the tensile strength and tensile modulus with reduced elongation at break compared to base polymer LDPE. The inclusion of OxPE in LDPE/C20A further enhances the tensile properties of nanocomposites. In the case of virgin LDPE, there was an increase of 53% for tensile strength and 66% for tensile modulus. Nevertheless, the crystallization temperature of the specimens increased significantly and the degree of crystallization in the nanocomposite increased with increasing coupling concentration. Substantial enrichment of flame retardant properties has been observed for ternary nanocomposites.

INTRODUCTION

Over the last few decades, the use of layered silicate nanoparticles, such as polymer-reinforced clay, has charmed much academic and industrial interest due to the expected improvement in properties. In nanotechnology, polymer nanocomposites consist of a polymer matrix filled with a layered silicate that dispersed at a nanoscale phase. When the elements are well-defined by their size, at least one of the three external dimensions is about 1 nm to 100 nm (1). Hybrid ingredients are formed by adding inorganic nanoparticles to the organic polymer matrix to form a class of polymer/clay nanocomposites. Generally, natural clay polymers are used as cheap raw components to manufacture nanocomposites due to their structural and availability. Inorganic nanoclay, which is commonly used, is montmorillonite, which has an aluminosilicate structure, with two tetrahedral silica sheets containing an octahedral alumina sheet. Polymer/clay nanocomposites exhibit higher mechanical properties (2-3), compressive gas permeability, increased solvent resistance, high thermal distortion temperature (HDT), and increased flame retardant properties (4-7) than virgin polymer. Improved properties, including many exfoliated clay dispersing polar groups, are achieved by allowing the clay to easily disperse into such polymer matrix (8), while some studies of nonpolar polymers, such as polyolefin (PP or PE) have found a lower degree of clay exfoliation in the polymer matrix due to

their hydrophilicity and poor interaction with the polar aluminosilicate surface of the clay (9).

Nanocomposite materials have gained important industrial interest and research endeavors to inspire the improvement of nanocomposite as well as other polymers. There are three ways to synthesize polyolefin/clay nanocomposites, namely situ polymerization, solution method and melt compounding method. From all of these, the melt compounding method is the simplest and most cost-effective way to manufacture nanocomposites. Polyethylene/organoclay nanocomposites are interested in the melt compounding process (10-11). Zhang et al. (12) reported that the flammability properties of polyethylene-clay nanocomposites have a significant reduction in peak release rate and also observed that polyethylene-clay nanocomposites have a mixed immiscible-intercalated structure. Natural montmorillonite, however, is hydrophilic so it is not compatible with many hydrophobic engineering polymers, as most polymer-layered silicates do not dispersed easily. To get over this problem, a simple cation exchange procedure is used to produce montmorillonite clay organophilic. Thus, interfacial interactions between the clay layer and the polyolefin matrix should be introduced to develop polymer nanocomposite with modified polar group called coupling agents or interfacial agents in nanocomposite structures (13). Maleic anhydride grafted polyolefin is commonly used as a compatibilizer. Many experimental results have shown the preparation and physical properties of manufactured polypropylene

nanocomposites of maleic anhydride grafted polypropylene (14-15). Polyethylene/organo-clays, on the other hand, are less exposed to nanocomposites due to their non-polar chain structure and lack of thermodynamic forces, which is a great challenge to achieve structure (16). In less research, some authors have suggested that low molecular weight (LMW) reactive compounds can be successfully used as a coupling agent for polyethylene nanocomposites (17-18). They suggested that these functional oligomeric compounds could easily disperse into clay galleries and cause an additional delamination because they have much greater mobility during nanocomposite processing than their high molecular weight. Literary data on the use of low molecular weight oxidized polythene (OxPE) as a coupling agent for polymer/clay nanocomposites are relatively rare. In this research, we used low molecular weight (LMW) OxPE as a coupling agent to manufacture LDPE/organo clay nanocomposite. OxPE is a modified, LMW polyethylene that has several functions, for example, mainly carboxylic acids, esters and ketones. It was used as a processing aid in some polymer blends as a coupling agent and coating formula. OxPEs have also been used in polymer blends as coupling agent. In the present study, the effects of coupling agent content and the clay dispersion on the morphological, mechanical, thermal and flame retardant properties of LDPE/organo clay nanocomposite were investigated.

EXPERIMENTAL

Materials and nanocomposite preparations

Granules of low-density polyethylene (LDPE) (density = 0.918 g/cm³, MI = 3 g/10 min) (trade name: Cosmoplene) were supplied by the Polyolefin Company, Private Ltd., Singapore. Low molecular weight oxidized polyethylene (molecular weight, M_n : 2950; acid number: 30) provided by Honeywell (AC[®] 330) was used as a coupling agent. Commercial organoclay Cloisite 20A (C20A) supplied Southern Clay Products. C20A was produced by cation exchange with 0.95 meq/g of dimethyl-dehydrogenated tallow ammonium chloride in sodium montmorillonite (Cloisite Na⁺, with a CEC of 0.926 meq/g). Tallow proportional (50%) may be a composition of unsaturated n-alkyl groups with approximate compositions: 65% C18, 30% C16, and 5% C14; hydrogenated tallow has only 3% unsaturation. The polymer and organoclay were dried in an air-circulating oven at a constant weight of 80°C. Compositions of LDPE/organo clay nanocomposite are listed in Table 1.

Table 1. Sample compositions.

Sample Code	LDPE (wt%)	OxPE (wt%)	Cloisite-20A (wt%)
LDPE	100	-	-
LC5	95	-	5
LC5O10	85	10	5
LC5O15	80	15	5
LC5O20	75	20	5

LDPE: Low-density polyethylene; OxPE: Low molecular weight oxidized polyethylene

The nanocomposites were made by mixing LDPE/5 wt% organoclay (LC5) and LC5/OxPE with 10, 15, and 20 wt% of OxPE using melt compounding in a co-rotating twin-screw extruder (Brabender Plasticorder, model: PLE-331). During polymer and organoclay loading, the rotor speed and temperature were maintained at 30 rpm and 180 °C, for 3 min, respectively, then gradually increased to 60 rpm. The general blending time was 10 min. After blending, the mixture was poured into a mold and therefore the molten nanocomposites were obtained by a hot compression-molding machine. The mixture was pressed at 10 MPa during a hydraulic press (Carver Laboratory Press, USA, Model 3856) at 190 °C for 10 min. After that, the nanocomposite sample containing steel plates was cooled to another press (Carver Laboratory Press, USA, Model 2518) operated at cooling condition. Films of 2 mm thickness were made and cut to standard sizes and shapes to test the mechanical properties.

Nanocomposite test

The morphology of nanocomposites in LDPE/C20A has been observed using transmission electron microscopy (TEM: JEM 2010 F) with an acceleration voltage of 200 kV. A Sorvall MT6000 microtome was accustomed to cut the skinny part (70 nm) of the specimen at room temperature.

The degree of intercalation or exfoliation was assessed with XRD. The XRD patterns were recorded employing a Philips X'pert MPD (40 kW, 30 mA) operating with Cu-K α radiation ($\lambda = 0.15406$ nm) at 40 kV and 30 mA within

the range of $2\theta = 1-10^\circ$ with a scan speed of $0.02^\circ/\text{s}$. Interlayer spacing of the silicate layers was determined using the peak positions according to Bragg's law: $d = \lambda/(2\sin\theta)$, where λ is the wave length, 0.154 nm, θ is the diffraction angle and d is the basal space between clay layers.

The tensile properties of virgin LDPE and LDPE/C20A nanocomposites were examined by tensile strength, tensile modulus, and elongation at break. Standard specimens were sampled from compression molded sheets and then conditioned at temperature of (25 ± 2) °C and relative humidity of $50 \pm 5\%$ for 24 h. To analyze the tensile properties of LDPE/C20A nanocomposites, the test was performed on a screw-driven universal testing machine (Instron-4466) equipped with 10 kN electronic load cells and mechanical grips at a crosshead speed of 30 mm/min according to ASTM standards. All values were measured 5 times to take the average value.

The thermal behavior of the specimens was analyzed by differential scanning calorimetry (DSC). Crystallization behavior of the specimens was performed on DSC-Mettler. In an aluminum crucible, a sample weighing about 5–8 mg was heated to 180 °C from room temperature with a heating rate of 10 °C/min and kept at this temperature for 5 min to remove the thermal history. It was then cooled to room temperature with a cooling rate of 10 °C/min and reheated to 180 °C with a heating rate of 5 °C/min. All heating and cooling runs were conducted under

a helium atmosphere at a flow rate of 25 ml/min. Melting peak temperature (T_m) and melting enthalpy (ΔH_m in J/g) were obtained from the second heat run. The degree of crystallinity (X_c %) was calculated using the melting enthalpy of the specimens in step with the subsequent equation:

$$X_c(\%) = \frac{\Delta H_m}{\Delta H_m^0} \times 100 \quad (1)$$

where ΔH_m^0 is the melting enthalpy of the 100% crystalline form of PE (279 J/g) (19)

The flammability of virgin LDPE and nanocomposites was assessed by ascertaining their limiting oxygen index (LOI). Measurements were performed using FTA flammability equipment, supplied by Stanton Redcroft, by ASTM D-2863. The burn rate was set to LOI = 21.8 as the length of the plate which burns for one second.

RESULTS AND DISCUSSION

Organoclay dispersion analysis

It is well known that the dispersion of fillers in the polymer matrix can have a significant influence on the mechanical properties of the nanocomposite. Dispersion filler in thermoplastics isn't an easy process. The problem is even more severe, when using nanoparticles as filler, because the nanoparticles have a strong tendency to agglomerate. Consequently, homogeneous dispersion of the nanoparticles in the thermoplastic matrix is a difficult process. A good dispersion can be achieved by adding a coupling agent such as OxPE. The dispersion of organoclay in

LDPE nanocomposite was also confirmed by TEM monitoring. Figure 1(a-d) displays TEM micrographs of LDPE/C20A nanocomposites consisting of 5 wt% C20A (designated as LC5), LDPE/5 wt% C20A/10 wt% OxPE (denoted as LC5O10), LDPE/5 wt% C20A/15 wt% OxPE (marked as LC5O15), and LDPE/5 wt% C20A/20 wt% OxPE (abbreviated as LC5O20). Figure 1 (a) shows the dispersion of C20A particles in LDPE matrix. It can be seen that most C20A particles form agglomerates in LDPE matrix due to the incompatibility between nanoparticles and LDPE matrix. The black shape represents the tactoids in C20A and the rest of the region represents an uninterrupted LDPE. Nevertheless, some black shapes may indicate some poorly dispersed C20A agglomerates. Figure 1 (b) on the other hand shows relatively fewer particles in C20A than in Figure 1 (a) and the C20A particles were separated into lighter parts by the method of mixing. Anyway, image exfoliated structures (white arrows) for LC5O15 (Figure 1 c) showed well-dispersed structures although several clay agglomerates and intercalated structures appeared simultaneously. Most C20A aggregates are broken down to primary particles. This should maximize the interfacial interaction between the C20A particles and the LDPE. This morphological monitoring by TEM was very consistent with other researchers (20). However, both unexfoliated clay tactoid and exfoliated platelets are present in Figure 1 (d). The LC5O20 sample has a large clay tactoid that correspond to intercalated structure. It can be clearly seen that the aspect ratio of clay layers in LC5O20 is higher than the

aspect ratio of LC5O15. The stiffness of these probes can be attributed to the dispersion of silicate layers, which can determine the polymer phases which increase the stiffness which increase the stiffness (21). These observations are supported by the results of the XRD analysis.

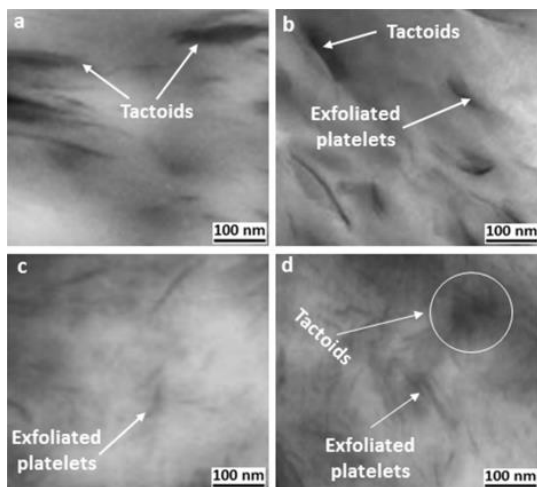


Figure 1 TEM images of nanocomposite samples: (a) LC5, (b) LC5O10, (c) LC5O15, and (d) LC5O20

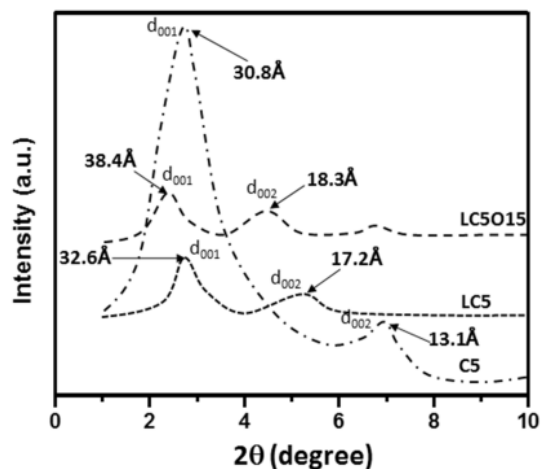


Figure 2 XRD patterns of 5 wt% C20A (C5), LDPE/5 wt% C20A (LC5) and LDPE/5 wt% C20A/15 wt% OxPE (LC5O15) nanocomposites

Dispersibility of clay layers in LDPE matrix

The structure of polymer/clay nanocomposites is conventionally described using X-ray diffraction (XRD). Due to the periodic arrangement of silicate layers, XRD is the most widely used technique for identifying clay-intercalated structures. The XRD patterns of cloisite 20A (C20A), LDPE/5 wt% C20A (LC5) and LDPE/5 wt% C20A/15 wt% OxPE (LC5O15) nanocomposites are shown in Figure 2. Two diffraction peaks are observed for the 5 wt% C20A (C5) corresponding to basal spacing of $d_{001} = 3.09 \text{ nm}$ ($2\theta = 2.86^\circ$) and $d_{002} = 1.31 \text{ nm}$ ($2\theta = 6.74^\circ$) by using the Bragg equation. The d_{001} plane reflection of LC5 without coupling agent is observed at $2\theta = 2.71^\circ$ corresponds to 32.6 \AA interlayer spacing. However, with adding OxPE, the peaks are shifted to lower angles in the nanocomposites. The d_{001} plane reflection of LC5O15 is observed at 2θ value of 2.29° , corresponding to 38.4 \AA (22). The peak height of the ternary nanocomposites (LC5O15) was very small, indicating an intercalated/exfoliated structure. This clearly indicates the strong intercalation/exfoliation capacity of OxPE in the silicate layers. The driving force of the intercalation arises from the hydrogen bonding between the acidic carboxyl group of OxPE and the oxygen groups of silicates.

Tensile properties of LDPE/organoclay nanocomposites

The mechanical properties of nanocomposites are directly related to the homogeneous clay dispersion and exfoliation or intercalation

of the polymer matrix. Interaction between exfoliated or intercalated nanoparticles and polymer matrix and large interfacial regions leading to high tensile strength, modulus and thermal stability. More uniform clay dispersion may result in higher strength and modulus but at the expense of distortion and toughness such as elongation at break and impact resistance. The tensile properties of LDPE, LDPE/5 wt% C20A (LC5), and LC5 nanocomposites with different coupling contents are illustrated in Figure 3. It was observed that when 5 wt % C20A (C5) was added to virgin LDPE, the tensile strength (TS) and tensile modulus (TM) of virgin LDPE increased with reduced elongation at break (Eb) and their value increased significantly as the OxPE content increased, but the Eb continuous declined. With C5 loading, the TS increased by about 22%, the TM enhanced by about 17% and the Eb reduced by about 30% compared to virgin LDPE. The increased tensile properties can also lead to a rich interfacial bond between the matrix and C5 due to the C5 long aliphatic chain leading to a rich interfacial bond between the matrix and C5. In general, the inclusion of organoclay in polymeric substances tends to reduce Eb. The results of Eb are illustrated in Figure 4. As seen in Figure 4, Eb of nanocomposites of the same C5 content followed this trend. Eb for nanocomposite samples decreased compared to LDPE. Typically, the filler causes a reduction in matrix deformation due to a role of mechanical barrier (23).

The OxPE load reinforcing facility has been well observed in this investigation. It's

interesting to determine how the OxPE was served in terms of the mechanical properties. The effect of OxPE load on the tensile properties of nanocomposites is shown in Figure 3. As can be seen in Figure 3, both TS and TM increased when adding OxPE with different content. OxPE nanocomposites exhibited a significant increase in TS compared to LC5 nanocomposites up to 15 wt% of OxPE loading and then decreased with increasing OxPE loading, while the TM of OxPE nanocomposites continuously increased up to 20 wt% of OxPE loading. The highest values obtained were 21.9 and 301 MPa, respectively, an increase of about 53% and 66% over virgin LDPE. Enhancement is achieved through strong hydrogen bonding between the -OH group of OxPE and the oxygen of silicate to the reinforcement of intercalated nanolayers, thereby increasing the inter-gallery space of the nanoclay (24). At higher OxPE loads, the tensile test showed a decrease in nanocomposites due to lower exfoliation and dispersion of nanocomposites. The increased tensile performance of the OxPE mixture (when compared to the unmodified system) is sometimes explained by the fine dispersion generated by the OxPE and by an improved solid-state adherence, which ends up in stress transfer at the dispersion phase from the matrix. Considering the tensile test results of the samples, we have concluded that enhancement in mechanical properties not only originated from the state of organoclay dispersion, but was also affected by the crystalline nature of the OxPE employed.

The TM of LDPE/5 wt% C20A/OxPE nanocomposites has improved dramatically with OxPE content. The increase in stiffness can be attributed to the dispersion of silicate layers, which can immobilize the polymer phases that stiffen the growth (21). In contrast, the tensile elongation at break of the LDPE/5 wt% C20A/OxPE nanocomposites is reduced with OxPE content. This reduction in Eb of the nanocomposites as compared with the unfilled polymer is attributed to the fact that fillers generally decreases the ductility of polymers and similar trends are also seen for nanocomposites (25). This suggests that the OxPE is effective in increasing adherence between C5 and LDPE molecular chains. A reduced Eb often means a reduced energy to break. In short, better tensile properties were obtained due to better exfoliation and good dispersion of C5 in the LDPE matrix.

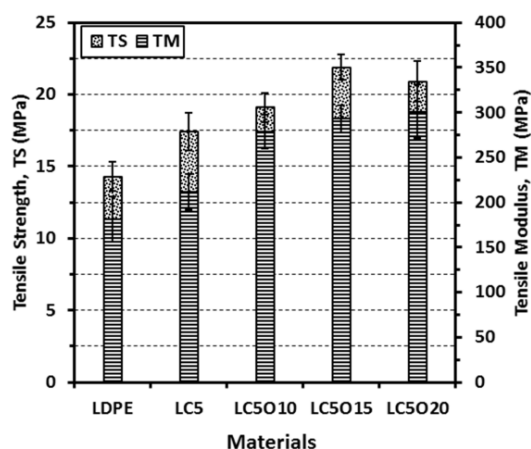


Figure 3 Tensile strength and modulus of virgin LDPE and its nanocomposites

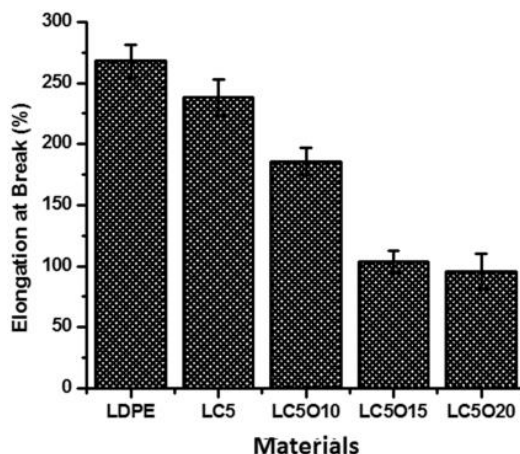


Figure 4 Elongation at break of virgin LDPE and its nanocomposites

Thermal properties of nanocomposites

Figure 5 (A) displays the crystallization exotherms of virgin LDPE, LC5, LC5O10, and LC5O15 nanocomposites recorded at a cooling rate of $10^{\circ}/\text{min}$ during the cooling cycle. The crystallization, melting peak temperatures and degree of crystallinity are tabulated in Table 2. This shows that the inclusion of organoclay and OxPE considerably changes the crystallization behavior of LDPE. As shown in Figure 5 (A), the crystallization peak temperature (T_c) of the samples shifted to a higher temperature than the virgin LDPE, with increasing the content of the OxPE. The T_c increased from 95.7°C of LDPE to 99.8°C of C5 nanocomposite. For LC5O10 sample, the T_c is increased up to 101.5°C . It's noteworthy that the T_c of the LC5O15 sample increased to 102.9°C , much larger than the LDPE and even larger than the LC5O10 nanocomposite. From Table 2, we can see that the melting peak temperature (T_m) has changed slightly with the increase in the content of the OxPE, and the T_m has increased slightly with increasing OxPE

content. This is responsible for the heterogeneous crystallization on the organoclay surface, which can develop the crystallization of LDPE, slightly increasing the T_m of the nanocomposite (26). The T_m of virgin LDPE, LC5, LC5O10, LC5O15 and LC5O20 nanocomposites are in the range 109.6 °C-111.4 °C. Compared to virgin LDPE, the T_m of nanocomposites is transferred at higher temperatures and the maximum T_m is obtained at LC5O15.

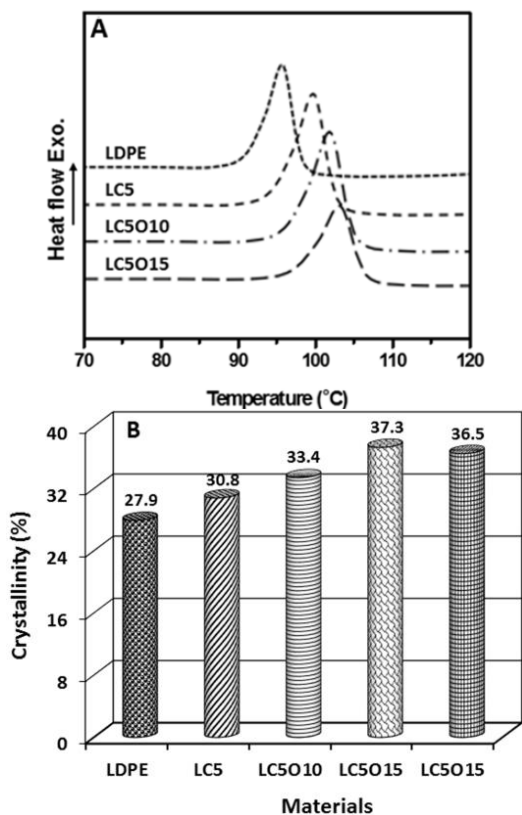


Figure 5 DSC (A) Crystallization exotherms and (B) crystallinity of virgin LDPE, LC5, LC5O10, LC5O15, and LC5O20 nanocomposites

Figure 5 (B) displays the variation in X_c (%) of the specimens. Influenced by the introduction of OxPE content in the nanocomposites of

LC5O10, LC5O15, and LC5O20, X_c was higher than virgin LDPE. The inclusion of organoclay and OxPE contents into semicrystalline polymers increases the crystallization rate, resulting in higher crystallinity and higher T_c . According to Zaman et al (2), the inclusion of organoclay and OxPE to the LDPE matrix increases the crystallization percentage.

Table 2 Thermal properties of virgin LDPE and its nanocomposites.

Sample code	T_c (°C)	T_m (°C)	ΔH_m (J/g)	X_c (%)
LDPE	95.7	109.6	77.8	27.9
LC5	99.8	109.9	85.9	30.8
LC5O10	101.5	110.5	93.1	33.4
LC5O15	102.9	111.4	104	37.3
LC5O20	102.6	111.1	101.8	36.5

Combustibility of the nanocomposites

The limiting oxygen index (LOI) is measured by the volumetric fraction of O_2 within the N_2 mixture, where the substances still burn, are:

$$LOI = O_2 / (O_2 + N_2)$$

The higher the LOI of a given material, the lower its combustibility. The LOI value of the specimens is displayed in Figure 6 (a). It's worth noting that the virgin polymer LDPE has a relatively high LOI. The LOI values of binary nanocomposites are only LC5 higher than that of virgin polymer components. Therefore, the presence of organoclay reduces the combustion of the polymer. LOI increased with OxPE content

increasing up to 15 wt% and then decreasing with increasing OxPE content. Furthermore, the presence of organoclay and the presence of OxPE lead to a significant reduction in the combustion rate of the substance up to 15 wt% (Figure 6 (b)). Nanocomposites exhibit burn retardant properties by creating a protective barrier to heat and mass transfer due to the accumulation of silicate and OxPE on the surface of the burning sample.

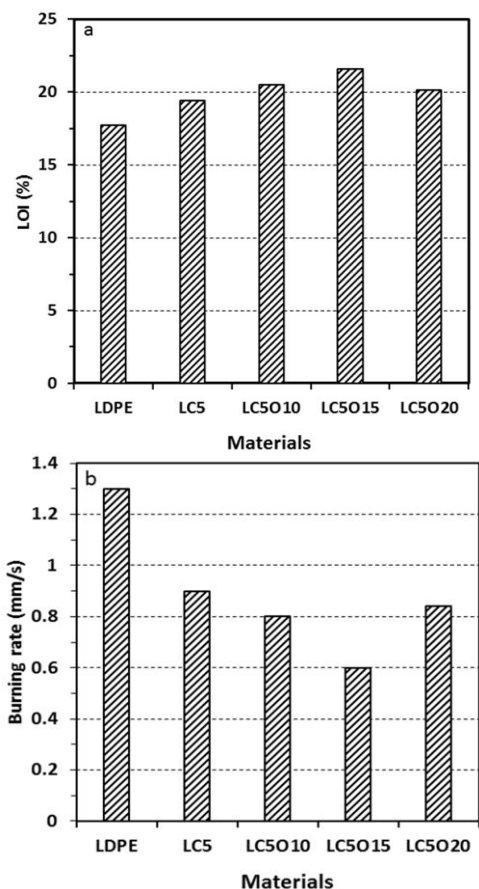


Figure 6 (a) Limiting oxygen index (LOI) of the virgin LDPE, LC5, LC5O10, LC5O15, and LC5O20 nanocomposites; (b) Burning rate of the virgin LDPE, LC5, LC5O10, LC5O15, and LC5O20 nanocomposites

CONCLUSIONS

In the present study, the tensile properties of LDPE/organoclay nanocomposites successfully manufactured by melt compounding method, using coupling agent (OxPE), were investigated. The characteristics of morphology, tensile properties, thermal behavior, and combustibility of LDPE/organoclay nanocomposites were examined by changes the inclusion of an OxPE. TEM photomicrographs exhibited that OxPE was effective in assisting the silicate platelet delamination. This outcome was also confirmed by the XRD of the specimens. The OxPE conferred higher tensile properties than control cases. DSC thermograms revealed that the crystallization temperature of the specimens increased significantly and the degree of crystallization in the nanocomposite increased with increasing OxPE concentration. However, melting and crystallization temperatures had a significant effect on blends and nanocomposites. The results show that LC5O15 nanocomposites have good flame retardant properties, which will be useful in terms of their application.

REFERENCES

1. Soundararajah Q, Karunaratne B, Rajapakse R. Montmorillonite polyaniline nanocomposites: Preparation, characterization and investigation of mechanical properties. *Mater Chem Phys.* 2009;113:850-55.
2. Zaman HU, Beg DH. Influence of two novel compatibilizers on the properties of LDPE/

- organoclay nanocomposites. *J Polym Eng.* 2014;34:75-83.
3. Zaman HU, Hun PD, Khan RA, Yoon K-B. Polypropylene/clay nanocomposites: Effect of compatibilizers on the morphology, mechanical properties and crystallization behaviors. *J Thermoplast Compos.* 2014;27:338-49.
 4. Bazmara M, Silani M, Dayyani I. Effect of functionally-graded interphase on the elasto-plastic behavior of nylon-6/clay nanocomposites; A numerical study. *Defence Technology.* 2021;17:177-84.
 5. Castro-Landinez JF, Salcedo-Galan F, Medina-Perilla JA. Polypropylene/ethylene and polar-monomer-based copolymers/montmorillonite nanocomposites: Morphology, mechanical properties, and oxygen permeability. *Polymers.* 2021;13:705.
 6. Singh VP, KK V, Sharma S, Kapur GS, Choudhary V. Polyethylene/sepiolite clay nanocomposites: effect of clay content, compatibilizer polarity, and molar mass on viscoelastic and dynamic mechanical properties. *J Appl Polym Sci.* 2017;134:45197.
 7. He W, Song P, Yu B, Fang Z, Wang H. Flame retardant polymeric nanocomposites through the combination of nanomaterials and conventional flame retardants. *Prog Mater Sci.* 2020;114:100687.
 8. Gómez-Aldapa CA, Velazquez G, Gutierrez MC, Rangel-Vargas E, Castro-Rosas J, Aguirre-Loredo RY. Effect of polyvinyl alcohol on the physicochemical properties of biodegradable starch films. *Mater Chem Phys.* 2020;239:122027.
 9. Depan D, Chirdon W, Khattab A. Morphological and chemical analysis of low-density polyethylene crystallized on carbon and clay nanofillers. *Polymers.* 2021;13:1558.
 10. Gill YQ, Song M, Abid U. Permeation characterization and modelling of polyethylene/clay nanocomposites for packaging. *Polym Bull.* 2020;77:3749-65.
 11. Wysocki S, Kowalczyk K, Paszkiewicz S, Figiel P, Piesowicz E. Green highly clay-filled polyethylene composites as coating materials for cable industry-A new application route of non-organophilised natural montmorillonites in polymeric materials. *Polymers.* 2020;12:1399.
 12. Zhang J, Wilkie CA. Preparation and flammability properties of polyethylene-clay nanocomposites. *Polym Degrad Stabil.* 2003;80:163-69.
 13. Seraji SM, Razavi Aghjeh M, Davari M, Salami Hosseini M, Khelgati S. Effect of clay dispersion on the cell structure of LDPE/clay nanocomposite foams. *Polym Composite.* 2011;32:1095-105.
 14. Lin TA, Lin M-C, Lin J-Y, Lin J-H, Chuang YC, Lou CW. Modified polypropylene/thermoplastic polyurethane blends with maleic-anhydride grafted polypropylene: Blending morphology and mechanical behaviors. *J Polym Res.* 2020;27:1-10.

15. Bakhtiari A, Ashenai Ghasemi F, Naderi G, Nakhaei MR. An approach to the optimization of mechanical properties of polypropylene/nitrile butadiene rubber/halloysite nanotube/polypropylene-g-maleic anhydride nanocomposites using response surface methodology. *Polym Composite*. 2020;41:2330-43.
16. Awad SA. Mechanical and thermal characterisations of low-density polyethylene/nanoclay composites. *Polymers and Polymer Composites*. 2020;10.1177/0967391120968441.
17. Kato M, Usuki A, Okada A. Synthesis of polypropylene oligomer—clay intercalation compounds. *J Appl Polym Sci*. 1997;66:1781-85.
18. Hasegawa N, Kawasumi M, Kato M, Usuki A, Okada A. Preparation and mechanical properties of polypropylene-clay hybrids using a maleic anhydride-modified polypropylene oligomer. *J Appl Polym Sci*. 1998;67:87-92.
19. Alamo R, Graessley W, Krishnamoorti R, Lohse D, Londono J, Mandelkern L. Small angle neutron scattering investigations of melt miscibility and phase segregation in blends of linear and branched polyethylenes as a function of the branch content. *Macromolecules*. 1997;30:561-66.
20. Durmus A, Kasgoz A, Macosko CW. Linear low density polyethylene (LLDPE)/clay nanocomposites. Part I: Structural characterization and quantifying clay dispersion by melt rheology. *Polymer*. 2007;48(15):4492-502.
21. Varghese S, Karger-Kocsis J. Natural rubber-based nanocomposites by latex compounding with layered silicates. *Polymer*. 2003;44:4921-27.
22. Fatma Isik C, Ulku Y. Preparation and characterization of low density polyethylene/ethylene methyl acrylate glycidyl methacrylate/organoclay nanocomposites. *J Appl Polym Sci*. 2011;120:3087-97.
23. Zhang MQ, Rong MZ, Friedrich K. Application of non-layered nanoparticles in polymer modification. In book: *Polymer Composites*. 2005; 25-44.
24. Rong MZ, Zhang MQ, Zheng YX, Zeng HM, Walter R, Friedrich K. Structure–property relationships of irradiation grafted nano-inorganic particle filled polypropylene composites. *Polymer*. 2001;42:167-83.
25. Paul DR, Robeson LM. Polymer nanotechnology: Nanocomposites. *Polymer*. 2008;49:3187-204.
26. Zaman HU, Beg MDH. Influence of two novel compatibilizers on the properties of LDPE/organoclay nanocomposites. *J Polym Eng*. 2014;34:75-83.